JOURNAL OF MATERIALS SCIENCE 29 (1994) 708–713

High-temperature creep and resultant anisotropy in ultrasonic velocity in isotropic graphite

M. NARISAWA*, M. ADACHI AND I. SOUMA
Government Industrial Research Institute of Osaka, Midorigaoka 1-8-31, Ikeda, Osaka 563, Japan

Plastic deformation of isotropic graphite in the vicinity of 2500 °C was studied using an Instron-type testing machine. The load–deflection curve was found to show a proportional limit at high temperature. Creep curves of graphite were also measured and were simulated by an empirical equation based on parabolic creep. Following the creep tests, ultrasonic velocity in the elongated graphite was measured. The velocity showed 5%–20% decrease after the creep. Below 2500 °C, the rate of velocity decrease along the elongation axis was always larger than that across the elongation axis. Above 2500 ° C, this behaviour was reversed with the rate of velocity decrease across the elongation axis being the larger. The rate of decrease appeared to depend firstly on temperature and secondly on stress.

1. Introduction

Recent developments in high-temperature technology require a better understanding of the properties of materials which have good high-temperature properties. In particular, carbon and graphite have been widely used as structural materials for furnaces, nuclear reactors and space planes in which superior toughness at high temperature is required. The mechanical properties of graphite materials at high temperature were vigorously studied during 1950s and 1960s. Many unique properties were found in high-temperature mechanical tests.

Elastic modulus and tensile strength of isotropic graphite increase as temperature increases, being opposite to ordinary materials [1–4]. The elastic modulus shows a maximum in the vicinity of 1800 °C [4] and the tensile strength shows a maximum in the vicinity of 2500 °C [1].

Creep of isotropic graphite at high temperature, above 2000 °C, has been also well studied. Early work suggested the existence of steady-state creep, as in ordinary metals after the initial state [1], but later works indicated that parabolic creep is common during the creep tests of graphite [5–10]. For the creep in pyrolytic graphite, the Nabarro–Herring mechanism was proposed, which was based on electron microscope observations [8–10]. However, the Nabarro–Herring mechanism is considered not to be appropriate in the case of isotropic graphite because the creep rate in isotropic graphite is proportional to the 5.5–8.0 power of applied stress, not to the 1.0–2.0 power. A dislocation mechanism is more probable than the Nabarro–Herring mechanism [6, 7, 10].

Any models for the creep of isotropic graphite, however, are rather tentative and speculative at present. In spite of several investigations, there are very few clues as to the origin of creep in graphite at high temperature. New methods are required to re-examine the graphite properties at high temperature.

In the former mechanical tests, loads have usually been applied through dead-weight constant-forcelever systems. In recent years, an Instron-type testing machine which can apply stress gradually to the specimen above 2000 °C has been developed [11]. By using this type of equipment, high stress can be applied to the graphite specimen without fracture, and the relationship between load and elongation can be clearly realized.

In addition, our group found recently that ultrasonic velocity in isotropic graphite showed an extreme decrease after high-temperature elongation. Based on this phenomenon, an imaging map of elongated graphite using the ultrasonic method was obtained [12]. The decrease in ultrasonic velocity is considered to be due to the decrease in elastic constants and is worthy of further attention because this phenomenon will add a new viewpoint to the creep of graphite.

In this study, the creep rates of isotropic graphite at high stress and high temperature were measured and simulated with an equation based on parabolic creep. Following the creep measurements, elongated parts were cut from the specimens and ultrasonic velocity along and across the elongation axis was measured. The relationship between the plastic deformation and the decrease in ultrasonic velocity, which must correlate with stress and temperature, is expected to provide

* *Present address:* College of Engineering, University of Osaka Prefecture, Gakuencho 1-1, Sakai, Osaka 593, Japan.

0022–2461

some clues as to the creep mechanism of isotropic graphite.

2. Experimental procedure

2.1. Specimen preparation

Isotropic graphite (IG-110, Toyo Tanso), was prepared for the mechanical tests at high temperature. Fig. 1 shows the shape of the specimen. The length of the specimen was 120 mm, its centre was machined to 10 mm diameter, and the length of the 10 mm diameter part was 10 mm. The specimen holders were also made of isotropic graphite.

2.2. Mechanical tests at high temperature

An Instron-type testing machine, mounted with a high-temperature furnace, was used for the mechanical tests. The temperature of the specimen was measured from the outside of the furnace using a radiation thermometer.

Before the tensile test, a small tensile stress was applied to the specimen and the temperature was raised to an appointed value over 3 h, keeping the stress fixed. After holding at the appointed temperature for 20 min, the fixed small stress was removed and the tensile test was carried out with a crosshead speed of 0.1 mm min^{-1}. It should be noted that the monitored deflection included not only the plastic deformation of the specimen but also the elastic deformation of the graphite holders.

For the creep test, the same procedures as for the tensile test were conducted. However, the stress maximum between 24.5 and 35 MPa was fixed at an appointed value by the fine adjustment of the crosshead position, while monitoring the elongation of the specimen. Because the stress is fixed, the monitored elongation is considered to include plastic deformation only. The creep test was continued for 1 h unless the sample broke prior to that. The monitored final elongation on a recorder in the furnace was almost the same as the results of direct measurement of the 10 mm diameter part with a pair of calipers, after removing the specimen from the furnace.

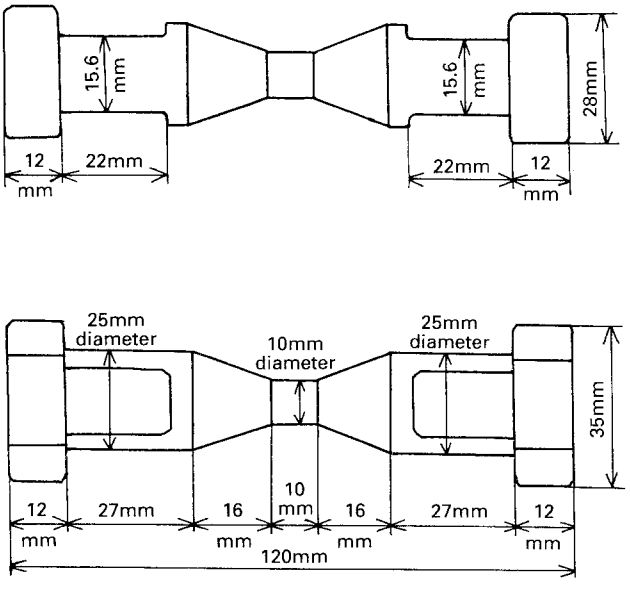

Figure 1 The shape of the test specimen.

2.3. Measurements of ultrasonic velocity

After the creep test, the 10 mm diameter part in the elongated specimen was cut to a cylinder shape and thinned to 6 mm along the diameter. The face-to-face planes in a sample were shaped parallel to each other.

Fig. 2 shows a block diagram of the ultrasonic immersion apparatus. The ultrasonic pulse passed from one transducer to another through the sample. All measurements were made in a water bath at room temperature, using 5 MHz transducers. The longitudinal wave velocity in the sample was calculated from the delay time of an observed pulse from a trigger pulse [13, 14]. The delay time of a pulse which has passed through water only was also measured at the same time, fixing the distance between the transducers. The longitudinal wave velocity in water was supposed to be 1.5×10^3 m s^{-1}. By changing the sample direction, the ultrasonic velocity along and across the elongation axis was obtained.

3. Results and discussion

3.1. Tensile tests of graphite at high temperature

Fig. 3 shows the results of tensile tests of isotropic graphite at high temperature. The horizontal axis

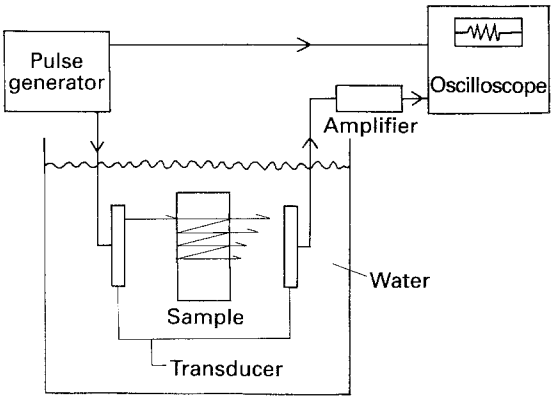

Figure 2 A block diagram of the ultrasonic immersion apparatus.

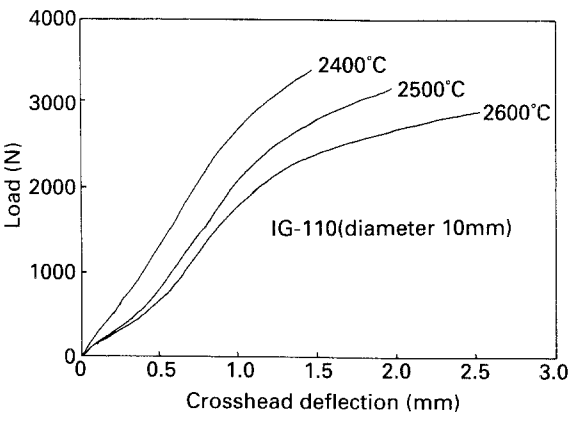

Figure 3 Load–deflection curves in the tensile tests of IG-110 at high temperature.

indicates the crosshead deflection, including deformation of the holders. All load–deflection curves tend to flatten in the high-stress region and the curves at 2500 and 2600 °C show proportional limits at 32 and 30 MPa. The observed nominal strength is 43 MPa at 2400 °C, 40 MPa at 2500 °C and 37 MPa at 2600 °C. These values are considerably lower than the true tensile strength because the fracture occurred mainly at the end of the 10 mm diameter part.

Such curves, having proportional limits, have not been observed in tensile tests of isotropic graphite, but are often encountered in stress–strain curves of metallic single or polycrystals at low temperature. The shape of the curves is explained in accordance with dislocation behaviour and work-hardening. The abrupt increase in stress before the proportional limit is considered to be an "exhaustion" region, in which a few dislocation sources, particularly large in length, are used up, while the plateau in the curve following the proportional limit corresponds to the region in which a large number of sources each generate a few dislocations [15]. In spite of several investigations of dislocations in graphite, dislocation sources, such as the Frank–Read source, have not been found in graphite [16–18]. However, the exhaustion and multiplication of dislocations are still considered for explaining the proportional limits in the tensile test.

3.2. Creep tests of graphite at high temperature

Fig. 4a–c show creep curves obtained for isotropic graphite at high temperature with varying stress. A continuously decreasing creep rate with time is seen, in the absence of a steady-state creep, and there is no evidence of a third-stage creep region. Some empirical equations have been proposed for simulating the creep curves of graphite [1, 6–10]. In order to analyse the present results, the following equation was adopted [10]

$$\varepsilon = At^{1/2} \tag{1}$$

where ε is the creep strain, t the time and A a parameter dependent on stress and temperature. This equation is simple and based on the idea that the creep rate decreases inversely as $t^{1/2}$. This equation is considered to represent one type of Andrade creep, while the creep strain in true Andrade creep is proportional to $t^{1/3}$ [19, 20].

In our measurements, ε and t were measured from the starting point at which the appointed stress was achieved. Because the stress was always applied gradually, the specimen must be somewhat elongated before the starting point and work-hardening must have already occurred. Thus ε and t in Equation 1 are replaced as shown in the following equations

$$\varepsilon = \varepsilon' + At_b^{1/2} \tag{2}$$

$$t = t' + t_b \tag{3}$$

where ε' and t' are the strain and time observed in our measurements, whereas ε and t are the actual strain and time. t_b is the supposed time lag between an

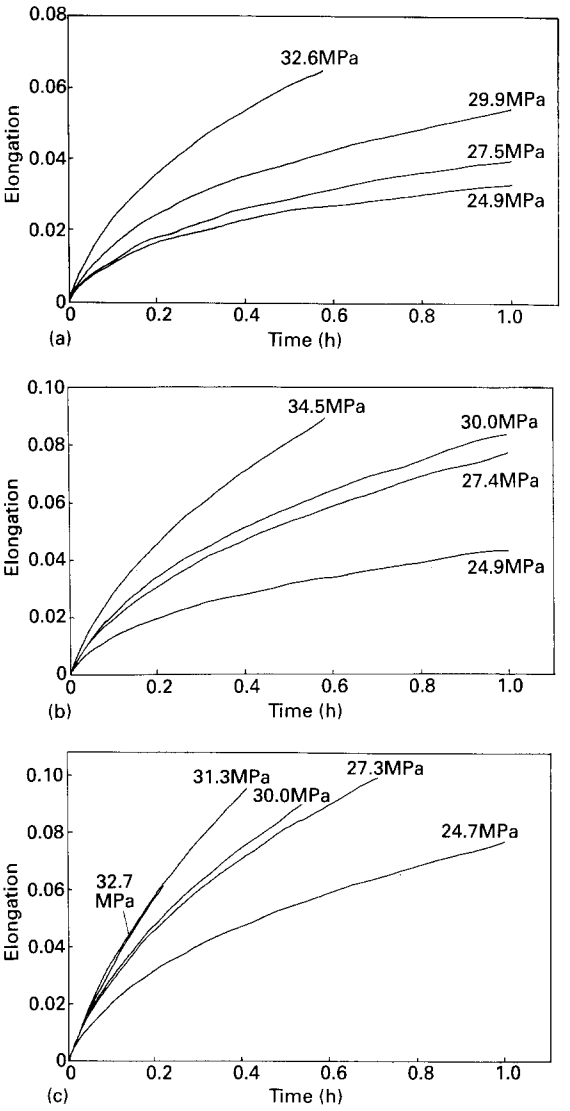

Figure 4 Creep strain versus time for IG-110 specimens at high temperature. (a) 2400 °C, (b) 2500 °C, (c) 2600 °C.

imaginary sudden stress point and the starting point. Although the actual stress was gradually applied, the values of t_b are available for estimating the rate of elongation and work-hardening before the starting point. Substituting Equations 2 and 3 into Equation 1, the following equation is obtained

$$t' = (1/A^2)\varepsilon'^2 + (2/A)t_b^{1/2}\varepsilon' \tag{4}$$

This equation contains only two parameters, A and t_b. Fig. 5a–c show the results of simulations of creep curves by Equation 4, picking up ten data points from each curve in Fig. 4. The observed curves at any stress and temperature are well simulated.

In Table I, calculated parameters, A, $t_b^{1/2}$ and t_b, obtained from the creep curves, are shown. $t_b^{1/2}$ shows small minus values at 24.9 MPa at 2400 and 2500 °C, indicating that the creep strain is not precisely proportional to $t^{1/2}$. A power of 0.4 or 0.45 of time will give better results. Adoption of a power of 0.4 or 0.45, however, complicates the equations. The quantity $t_b^{1/2}$ is so small that the 1/2 power is considered to be acceptable.

The calculated t_b values are usually adequate from 0–100 s. High t_b values at high stress at 2600 °C may

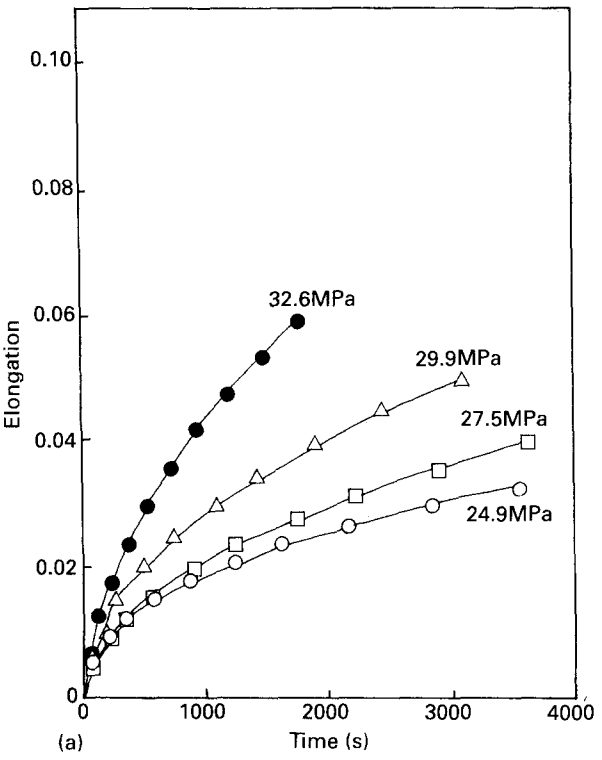

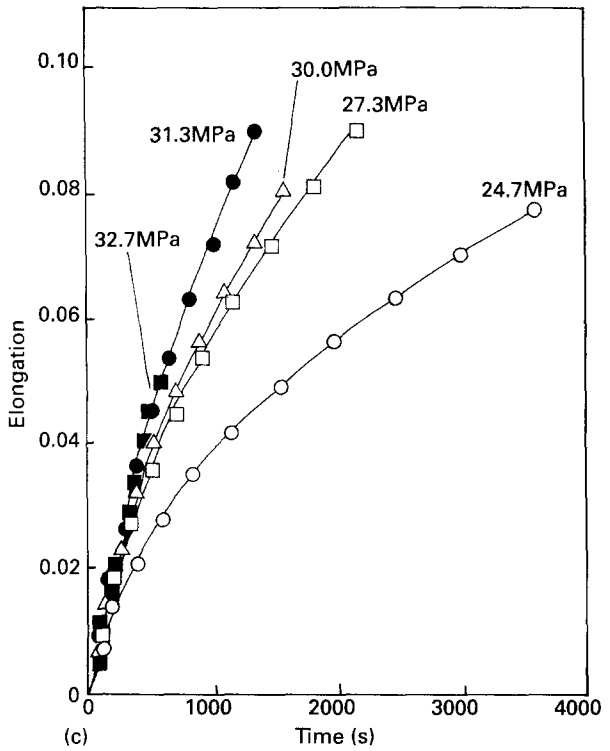

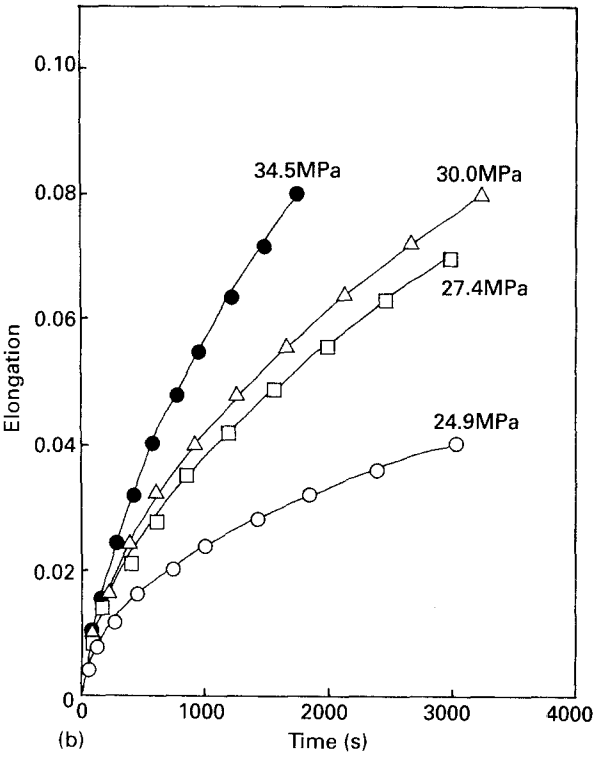

Figure 5 The results of simulation for creep curves of IG-110 at high temperature. (a) 2400 °C, (b) 2500 °C, (c) 2600 °C.

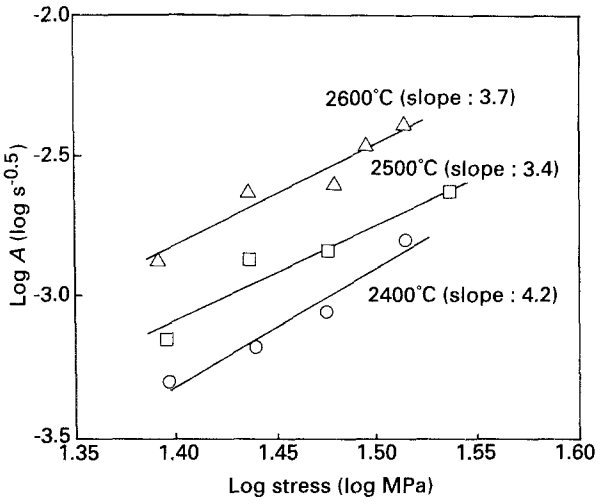

Figure 6 The stress-dependence of A at high temperature.

be caused by steady-state creep or fracture; this is ambiguous at present.

Fig. 6 shows the relationship between A and stress at each temperature. A tends to increase with increasing stress, being empirically proportional to the 3.4–4.2 power of stress. The coefficient of Andrade creep in metals also depends on stress and temperature but the relationship has not been clearly established [15, 19, 20].

Graphite is known to deform easily by slip along its basal plane, but such slip contributes only two independent slip systems [5]. Because general deformation in polycrystalline material requires cooperative slip by

TABLE I Calculated parameters from the results of simulation

Temperature (°C)	Stress (MPa)	$A(s^{-0.5})$	$t_b^{0.5}(s^{0.5})$	$t_b(s)$
2400	24.9	5.29×10^{-4}	−3.66	–
	27.5	6.73×10^{-4}	0.183	0.033
	29.9	9.23×10^{-4}	0.783	0.612
	32.6	1.63×10^{-3}	5.52	30.5
2500	24.9	7.23×10^{-4}	−0.564	–
	27.4	1.40×10^{-3}	5.04	25.4
	30.0	1.53×10^{-3}	5.14	26.4
	34.5	2.34×10^{-3}	8.07	65.2
2600	24.7	1.37×10^{-3}	3.86	14.9
	27.3	2.32×10^{-3}	8.35	69.7
	30.0	2.56×10^{-3}	10.0	100
	31.3	3.45×10^{-3}	13.2	173
	32.7	4.14×10^{-3}	18.8	352

five independent systems, void or crack formation with some volume change is unavoidable in the creep of graphite. However, void formation is not considered to be the rate-controlling process, because the increase in average stress with void formation would cause the creep rate to increase rather than decrease during the creep test. Furthermore, the slip along the basal plane is so easy even at low temperature that it cannot be the only rate-controlling process above 2000 °C. Other deformation mechanisms, such as non-basal plane slip, or grain-boundary sliding, must operate in conjunction with void formation and the basal plane slip

3.3. Ultrasonic velocity in elongated graphite

Fig. 7 shows the relationship between the stress and ultrasonic velocity in the specimens elongated by the creep tests. The velocity was measured after cooling and removing the specimens from the furnace [12]. The measured velocity always decreases with elongation, and the rate of decrease appears to depend on stress on the specimens at high temperature. A large stress tends to cause a large decrease in velocity.

The temperature dependence of the ultrasonic velocity is more remarkable than the stress dependence. In the elongation at 2400 °C, the ultrasonic velocity along the elongation axis is always lower than the ultrasonic velocity across the elongation axis. On the other hand, the ultrasonic velocity across the elongation axis is always lower than that along the elongation axis in the elongation at 2600 °C. After elongation at 2500 °C, the ultrasonic velocity decreases almost isotropically.

The ultrasonic velocity is known to be related to the dynamic elastic constant of the materials [13, 14]. Oku and Eto [21, 22] found compressive prestress on isotropic graphite at room temperature diminished the ultrasonic velocity, and emphasized the role of crack formation in the velocity decrease, particularly at high pressures.

In the case of graphite, however, the oscillation of basal dislocations between pinning points is known to diminish the shear modulus of single crystals [18, 23]. If the basal dislocations in isotropic graphite [24] are multiplied in the process of creep tests. The decrease in ultrasonic velocity can be explained as being due to a decrease in shear modulus in the graphite crystallite. Although basal dislocations cannot directly influence the high-temperature creep, they are considered to play an important role in graphite elasticity. As stated before, no types of dislocation source, basal or non-basal, have been found in graphite. However, the mechanism based on basal dislocations in isotropic graphite is more probable than crack formation for explaining the decrease in ultrasonic velocity after high-temperature creep.

It is generally known that the tensile strength of isotropic graphite shows a maximum in the vicinity of 2400–2500 °C [1]. This temperature is very consistent with the region in which the ultrasonic velocity along the elongation axis becomes almost the same as the velocity across the elongation axis. This suggests that

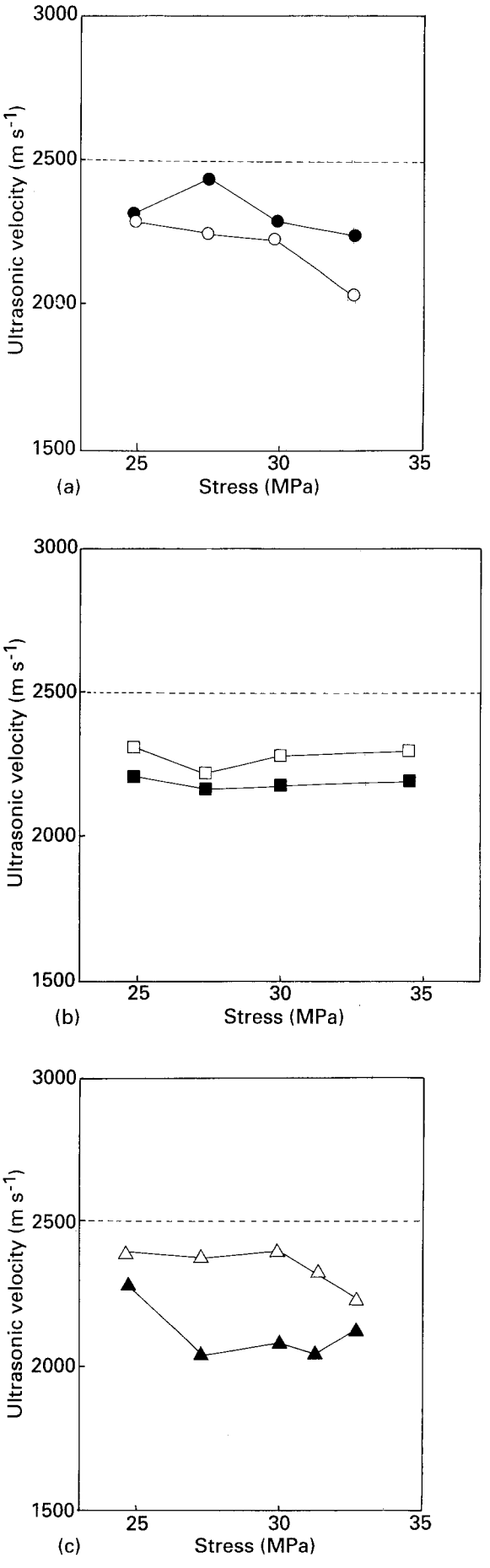

Figure 7 The relationship between stress and ultrasonic velocity in IG-110 after the creep tests. (— — —) The original ultrasonic velocity. (a) 2400 °C, elongated (○) along the elongation axis, (●) across the elongation axis. (b) 2500 °C, elongated (□) along the elongation axis, (■) across the elongation axis. (c) 2600 °C, elongated (△) along the elongation axis, (▲) across the elongation axis.

the graphite crystallite, which contains the basal plane dislocations, begins to flow and orient above 2500 °C.

4. Conclusions

A proportional limit, as in ordinary metals, appeared in the high-temperature load–deflection curve for isotropic graphite, indicating the occurrence of two types of elongation at high temperature. The creep curve was simulated by an empirical equation which contains only two parameters, A and t_b. The results of the simulation are quite good and indicate the existence of typical work-hardening in the plastic deformation of graphite. The ultrasonic velocity in the deformed graphite always decreased. The velocity along the elongation axis was lower than that across the elongation axis at 2400 °C, whilst the opposite was observed at 2600 °C, At 2500 °C, the ultrasonic velocity decreased isotropically. The decrease in velocity is considered to be due to the multiplication of the basal dislocations in the graphite crystallites. The process of non-basal plane slip or grain-boundary sliding, accompanied by basal dislocation multiplication, is considered to be the rate-controlling process of graphite creep at high temperature.

Acknowledgements

The authors thank Mr K. Niwa for help with the mechanical tests of graphite at high temperature, and Mr I. Ogino for his advice on taking the ultrasonic measurements. Thanks are also due to Dr Y. Sawada for helpful discussion, Professor K. Okamura, University of Osaka prefecture, for advice on the mechanical properties of refractory materials, and Professor T. Tsuzuku, Nihon University, for his comments on dislocation behaviour in graphite.

References

1. C. MALMSTROM, R. KEEN and L. GREEN Jr, *J. Appl. Phys.* **22** (1951) 593.
2. L. GREEN Jr, *J. Appl. Mech.* **20** (1953) 289.
3. I. B. MASON and R. H. KNIBBS, *Nature* **188** (1960) 33.
4. J. F. ANDREW and S. SATO, *Carbon* **1** (1964) 225.
5. E. G. ZUKAS and W. V. GREEN, *Nature* **212** (1966) 1454.
6. W. V. GREEN and E. G. ZUKAS, *Electrochem. Tech.* **5** (1967) 203.
7. E. G. ZUKAS and W. V. GREEN, *Carbon* **6** (1968) 101.
8. W. V. KOTLENSKY, *ibid.* **4** (1966) 209.
9. G. M. JENKINS, *ibid.* **7** (1969) 9.
10. G. M. JENKINS, in "Chemistry and Physics of Carbon 11" (Marcel Dekker, 1973) p. 189.
11. S. SATO, A. KURUMADA, H. IWAKI and Y. KOMATSU, *Carbon* **27** (1989) 791.
12. M. NARISAWA, M. ADADHI and I. SOUMA, *ibid.* **30** (1992) 815.
13. R. E. SMITH, *J. Appl. Phys.* **43** (1972) 2555.
14. D. E. SOULE and C. W. NEZBEDA, *ibid.* **39** (1968) 5122.
15. N. F. MOTT, *Philos. Mag.* **44** (1953) 742.
16. S. AMELINCKX and P. DELAVIGNETTE, *Phys. Rev. Lett.* **5** (1960) 50.
17. S. AMELINCKX and P. DELAVIGNETTE, *J. Appl. Phys.* **31** (1960) 2126.
18. C. BAKER and A. KELLY, *Philos. Mag.* **9** (1964) 927.
19. E. N. da C. ANDRADE, *ibid.* **7** (1962) 2003.
20. P. FELTHAN and J. D. MEAKIN, *Acta Metall.* **7** (1959) 614.
21. T. OKU and M. ETO, *Carbon* **11** (1973) 639.
22. M. ETO and T. OKU, *ibid.* **29** (1991) 11.
23. E. J. SELDIN and C. W. NEZBEDA, *J. Appl. Phys.* **41** (1970) 3389.
24. T. TSUZUKU, *Carbon* **1** (1963) 25.

Received 3 November 1992
and accepted 4 June 1993